Active Brownian motion tunable by light

2012 J. Phys.: Condens. Matter 24 284129

(http://iopscience.iop.org/0953-8984/24/28/284129)

IOP PUBLISHING JOURNAL OF PHYSICS: CONDENSED MATTER
J. Phys.: Condens. Matter **24** (2012) 284129 (6pp) doi:10.1088/0953-8984/24/28/284129

Active Brownian motion tunable by light

Ivo Buttinoni[1], Giovanni Volpe[1,2,4], Felix Kümmel[1], Giorgio Volpe[3] and Clemens Bechinger[1,2]

[1] 2. Physikalisches Institut, Universität Stuttgart, Pfaffenwaldring 57, 70569 Stuttgart, Germany
[2] Max-Planck-Institut für Intelligente Systeme, Heisenbergstraße 3, 70569 Stuttgart, Germany
[3] ICFO-Institut de Ciencies Fotoniques, Mediterranean Technology Park, 08860, Castelldefels (Barcelona), Spain

E-mail: giovanni.volpe@fen.bilkent.edu.tr

Received 11 October 2011, in final form 2 February 2012
Published 27 June 2012
Online at stacks.iop.org/JPhysCM/24/284129

Abstract
Active Brownian particles are capable of taking up energy from their environment and converting it into directed motion; examples range from chemotactic cells and bacteria to artificial micro-swimmers. We have recently demonstrated that Janus particles, i.e. gold-capped colloidal spheres, suspended in a critical binary liquid mixture perform active Brownian motion when illuminated by light. In this paper, we investigate in more detail their swimming mechanism, leading to active Brownian motion. We show that the illumination-borne heating induces a local asymmetric demixing of the binary mixture, generating a spatial chemical concentration gradient which is responsible for the particle's self-diffusiophoretic motion. We study this effect as a function of the functionalization of the gold cap, the particle size and the illumination intensity: the functionalization determines what component of the binary mixture is preferentially adsorbed at the cap and the swimming direction (towards or away from the cap); the particle size determines the rotational diffusion and, therefore, the random reorientation of the particle; and the intensity tunes the strength of the heating and, therefore, of the motion. Finally, we harness this dependence of the swimming strength on the illumination intensity to investigate the behavior of a micro-swimmer in a spatial light gradient, where its swimming properties are space-dependent.

(Some figures may appear in colour only in the online journal)

In recent years, active Brownian motion has attracted a lot of interest from biologists and physicists alike [1]. Unlike simple Brownian particles, whose motion is dominated by random fluctuations, active Brownian particles feature an interplay between random fluctuations and active swimming. While Brownian particles are at thermal equilibrium with their environment, active Brownian particles are capable of taking up energy and converting it into directed motion in a process that drives them out of equilibrium [2, 3].

A paradigmatic example of active Brownian motion is the swimming of bacteria such as *Escherichia coli* [4]. While the details may differ depending on the specific bacterial type, their motion can be generally described as a sequence of roughly straight trajectories (runs) and diffusive events (tumbles). Furthermore, bacteria can adapt their motion to the environmental conditions, thus optimizing their survival chances. In the presence of a nutrient gradient, for example, bacteria are able to move towards the regions with a higher nutrient concentration by adjusting the frequency of their tumbles [5], employing a food searching strategy that has been demonstrated to be optimal when the targets are diluted, sparse and able to regenerate [6].

In recent years much effort has been devoted to realizing artificial micro-swimmers [1]. Such micro-swimmers hold tremendous potential as autonomous agents to localize, pick up and deliver nanoscopic objects, e.g. in bioremediation, drug delivery and gene therapy [7–11]. Various approaches have been proposed in order to propel such artificial micro-swimmers [1]. For example, micro-swimmers composed of DNA-linked magnetic colloidal beads have been powered by external rotating magnetic fields which allows the

[4] Present address: Department of Physics, Bilkent University, Cankaya, Ankara 06800, Turkey.

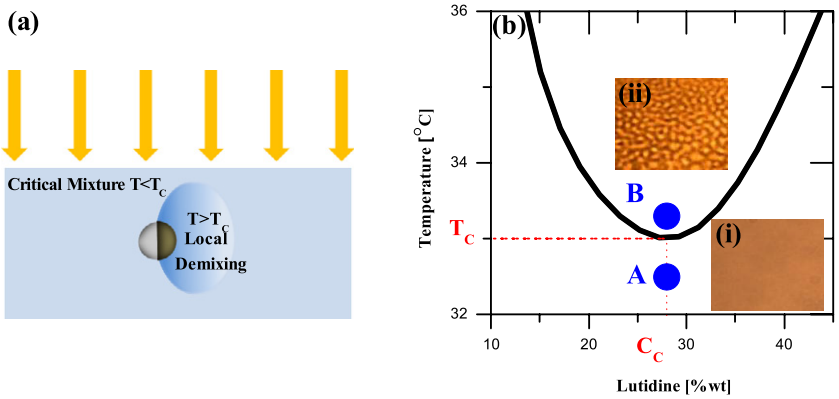

Figure 1. Active Brownian micro-swimmers in a critical binary mixture. (a) Schematic explaining the self-propulsion mechanism: a Janus particle is illuminated and the cap is heated above T_c inducing a local demixing that eventually propels the particle. (b) A schematic phase diagram for water–2,6-lutidine. The insets are bright-field microscopy pictures of the mixed (i) and the demixed (ii) phase at the critical concentration.

fabrication of swimmers [12–14], artificial flagella [15] or helical artificial tails [16]. Additionally, swimmers with a low Reynolds number have been powered using optical traps [17]. Although the motion of such micro-swimmers is not autonomous but controlled by the geometry and direction of external fields, the clear advantage of such approaches is that this motion can be kept going forever. A different approach deals with micro-swimmers capable of autonomous motion, mimicking more closely biological entities. The main difficulty is related to the need for a constant energy (fuel) supply that the micro-swimmers have to take up from their surroundings. Various kinds of Janus particles driven by self-phoretic forces have been particularly successful [18]. Such forces are produced by a chemical (self-diffusiophoresis [19–27]), electrical (self-electrophoresis) or thermal (self-thermophoresis [28]) gradient that the particle is able to generate around itself. For instance, Janus spheres or rods half coated by platinum and immersed in water enriched by hydrogen peroxide are propelled by a catalytic chemical reaction on the metallic surfaces [19, 21, 23]. However, since the hydrogen peroxide is continuously decomposed, it is necessary to adopt special experimental configurations in order to maintain a constant activation of the particles [26]. Self-thermophoretic micro-swimmers have also been demonstrated using gold-capped Janus particles immersed in water [28]. The thermophoresis occurs because the particles experience a local temperature gradient due to the light absorbed by the gold caps under illumination by a slightly focused laser beam.

Very recently, we presented a novel type of micro-swimmer whose active motion relies on the local demixing of a binary mixture, which is achieved by the local heating of Janus particles with light (figure 1(a)) [29]. This system avoids the above mentioned fueling problem and has even allowed us to study active Brownian motion in patterned environments. So far, however, the origin of the propulsion mechanism has not been studied in detail. In this paper, we investigate this swimming mechanism in more detail, showing that the local asymmetric demixing induced by the illumination-borne heating generates a local spatial chemical concentration gradient which is eventually responsible for the particle's self-diffusiophoretic motion. We study this effect as a function of the functionalization of the gold cap, the particle size and the illumination intensity. We finally study a situation where the self-diffusiophoretic motion is spatially inhomogeneous by using an illumination gradient.

The micro-swimmers used in our experiments consist of silica spheres (SiO_2, Microparticles GmbH, Germany) with different radii ($R = 0.5,\ 1,\ 2.13\ \mu$m). One side of these spheres is coated by thermal evaporation with a thin adhesion layer of chromium (2 nm) and, subsequently, with a thicker layer of gold (20 nm). In order to control which component of the mixture is preferentially adsorbed at the gold surface, we render it either hydrophilic or hydrophobic by chemical functionalization with thiols terminated with either polar (11-mercapto-undecanoic acid) or nonpolar (1-octadecanethiol) end groups. These Janus particles are then diluted in a critical binary mixture of water and 2,6-lutidine [30]. In figure 1(b) a schematic phase diagram of the mixture is shown. At the critical composition (0.286 mass fraction of lutidine) and below the lower critical temperature ($T_c = 307$ K) the mixture is homogeneous, as shown by the bright-field picture in inset (i) of figure 1(b). Increasing the temperature above T_c, the mixture separates via spinodal decomposition as shown in inset (ii) of figure 1(b). The bicontinuous wormlike structure is typical of the spinodal decomposition and has been observed not only in binary fluids [31, 32], but also during the phase separation of metallic alloys [33], glass alloy systems and polymeric blends with high molecular weight [34, 35].

The temperature of the critical suspension is kept a fraction of a degree below the critical point with a flow thermostat (point A in figure 1(b)). The whole sample ($170 \times 130\ \mu$m) is then illuminated with green light at $\lambda = 532$ nm near the plasmonic absorption peak of gold [36]. Due to light absorption, the gold caps are heated above T_c; the temperature at the silica side does not change because silica does not absorb green light. Thus, the illumination triggers the heating of the caps and, subsequently, the local demixing of the critical mixture. In our experiments,

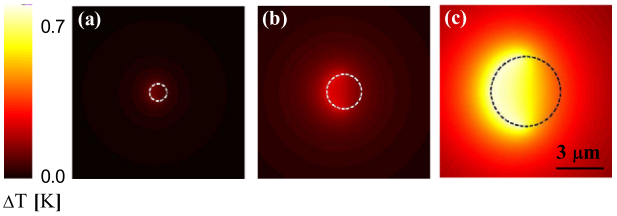

Figure 2. Light-induced heating. Numerical simulations of the temperature increase ΔT in the equatorial plane of a Janus particle with $R =$ (a) 0.5, (b) 1 and (c) 2 μm. In all cases, the dashed line profiles the contour of the particle, the cap is on the left side and $I = 1\ \mu\text{W}\ \mu\text{m}^{-2}$.

homogeneous illumination is obtained by rapidly scanning a highly defocused (spot radius $\approx 30\ \mu$m) laser beam over the entire area of the sample using an acousto-optical deflector. The light intensity is kept lower than $\approx 10\ \mu\text{W}\ \mu\text{m}^{-2}$ in order to rule out optical forces, which are typically relevant only for I at least an order of magnitude larger.

In order to better understand the heating process induced by the illumination, we have numerically estimated the temperature increase ΔT for an incident light intensity comparable with the experimental values. Heat is generated only in the cap because of the absorption associated to the imaginary component of the dielectric constant of gold [36], and then diffuses in the surrounding medium, i.e. silica sphere and water–2,6-lutidine, according to the Poisson heat equation. We followed in more detail the approach outlined in [37]: by applying the green dyadic method [38], we could estimate the electric field **E** inside the gold cap under uniform plane-wave illumination; then we derived the heat power Q generated at the cap, whose temperature is assumed to be uniform due to the high heat conductivity of the gold; finally, we calculated how Q diffuses in the surrounding medium using the Poisson heat equation and the heat conductivity of silica and water–2,6-lutidine. We note that ΔT is independent of the base temperature of the mixture. Figure 2 shows the results of the simulation of ΔT in the equatorial plane of a Janus particle with $R = 0.5$ (figure 2(a)), 1 (figure 2(b)) and 2 μm (figure 2(c)) illuminated with green (532 nm, linearly polarized) light of $I = 1\ \mu\text{W}\ \mu\text{m}^{-2}$; brighter colors correspond to a larger ΔT. The particles, whose contours are indicated by the dashed lines, are oriented so that the caps points to the left. As the particle size increases, ΔT becomes larger, because of the larger dissipation at the gold cap. More interestingly, we notice that ΔR is strongly asymmetric for all three particle sizes and that a sharp temperature transition occurs at the edge between the capped and uncapped sides of the particle; this asymmetry is responsible for the localization of the demixing at the cap side, for the instauration of a chemical gradient across the particle and, eventually, for the micro-swimmer's self-propulsion.

When the temperature locally increases above T_c, the binary mixture locally demixes and generates a demixed region around the Janus particle. In order to understand how this demixing fuels the particle's directed motion, we need to visualize its size and shape. Therefore, we added a fluorescent dye (Rhodamine 6G), which preferentially dissolves in lutidine, to the mixture and mapped the resulting fluorescence intensity. In figure 3, we show the fluorescence intensity encoded in color, i.e. yellow (red) for high (low) fluorescence intensity. Figure 3(a) shows the concentration of lutidine around a Janus particle with a hydrophilic-functionalized cap. The cap is easily identified as the bright half-moon shape at the center of the picture. Upon illumination, the lutidine becomes depleted from the area near the cap (red, water-rich phase), while it accumulates at the silica side (yellow, lutidine-rich phase), which is hydrophobic (in comparison to the hydrophilic-functionalized cap), thus resulting in a concentration gradient around the particle. The particle moves within this gradient in the direction of the lutidine-rich phase as indicated by the black arrow. Figure 3(b) shows the lutidine concentration around a Janus particle with a hydrophobic cap. In this case, the lutidine-rich phase (yellow) accumulates at the cap, while the water-rich (red) phase gets depleted and accumulates at the silica side, the latter being more hydrophilic than the cap. Again, the particle moves in the resulting gradient towards the lutidine-rich phase (arrow). These measurements confirm self-diffusiophoresis as the driving mechanism for the observed active motion. In order to rule out other possible mechanisms of self-propulsion, in particular self-thermophoresis, we repeated these measurements in pure water; here, we did not observe any directed motion under illumination intensities comparable those used in our experiments.

After having investigated the driving mechanism, we studied the motion of such micro-swimmers by injecting a diluted suspension in a thin glass cell ($\approx 100\ \mu$m high). Owing to gravity, the particles sediment to the bottom of the sample cell and their motion is effectively constrained to two dimensions (for the illumination intensities considered in this work). We recorded movies at 7.5 frames s^{-1} and employed digital video microscopy to track the particle trajectories at different illumination intensities. When the sample is kept at a temperature far from T_c, i.e. $\Delta T \gg 1$ K, the local illumination-induced heating is not sufficient to cross the spinodal line and, therefore, to induce a local demixing. On increasing the illumination intensity, the trajectories remain Brownian with a diffusion coefficient thus given by the Stokes–Einstein formula $D_{\text{SE}} = \frac{k_B T}{6\pi\eta R}$, where η is the binary fluid viscosity [30] and k_B is the Boltzmann constant. When the base temperature of the sample is kept very close to T_c, i.e. $\Delta T \approx 0.1$ K, the local heating is strong enough to cross the spinodal line and, thus, to induce a local demixing and to propel the particle. For smaller particle sizes, due to the lower heat power, higher illumination intensities are required, in agreement with the results from the simulations presented in figure 2.

The resulting motion is characterized by a crossover from ballistic motion at short times to enhanced diffusion at longer times, the latter due to random changes in the swimming direction [24, 26, 39]. The corresponding average particle speed v along the short-time ballistic runs, and the crossover time τ from the ballistic to the diffusive regime, can be estimated from the mean square displacement (MSD) [29]. Figure 4 shows the resulting values. The values of v as a

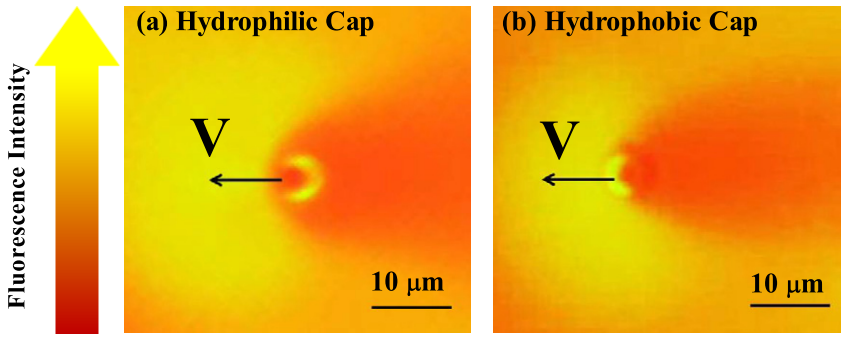

Figure 3. Demixed regions around illuminated Janus particles. (a) Distribution of the lutidine-rich phase (yellow), labeled with a hydrophobic dye (Rhodamine 6G), around a Janus particle with a hydrophilic gold cap (bright half-moon shape) under illumination. (b) Same as (a) for a Janus particle with a hydrophobic gold cap. Since the size of the demixed regions depends on the illumination intensity, the latter is set significantly higher than in the other experiments we present (10 μW μm^{-2}) in order to better visualize the gradient.

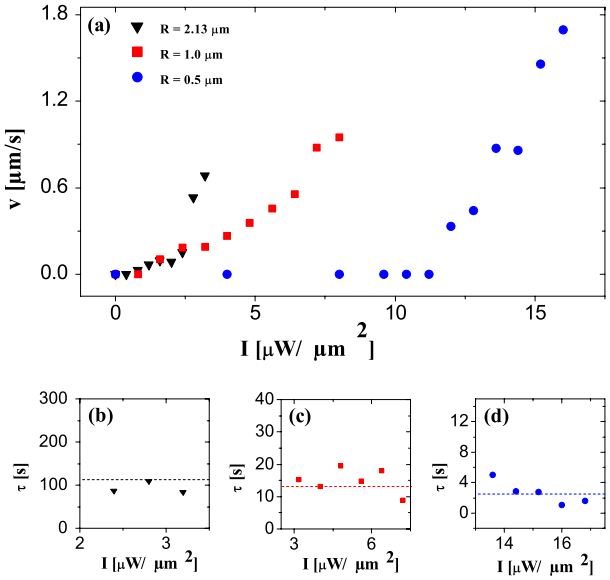

Figure 4. (a) Velocity (v) of self-propelled Janus particles as a function of the illumination intensity. (b)–(d) Crossing time (τ) for particles with radius $R =$ (b) 2.13, (c) 1.0 and (d) 0.5 μm.

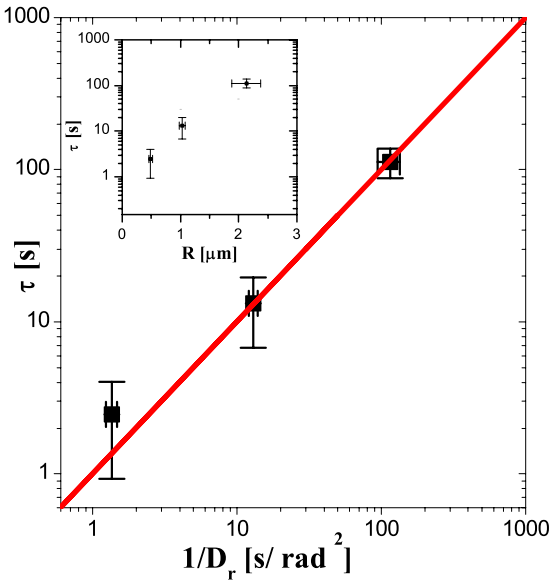

Figure 5. Crossing time τ from the ballistic to the diffusive regime plotted as a function of the rotational diffusion time $\tau_r = 1/D_r$ over two orders of magnitude. The inset shows the τ plotted as a function of the particle radius. The error bars are obtained from the measurements at different I.

function of I are plotted in figure 4(a), where the black triangles correspond to $R = 2.13$ μm, the red squares to $R = 1.0$ μm and the blue circles to $R = 0.5$ μm. Clearly, active Brownian motion, i.e. $v > 0$, sets in only above a certain illumination intensity threshold, which is higher for smaller particles due to their lower heat power (see also figure 2). This threshold can clearly be associated with the minimal heating necessary to cross the spinodal line where phase separation of the mixture occurs.

The values of τ are shown in figures 4(b), (c) and (d) for $R = 2.13$, 1.0 and 0.5 μm, respectively. It is evident that smaller micro-swimmers tend to change direction much more frequently. Interestingly, the values of τ for a given particle size are almost independent of the illumination intensity. These fitted values of τ agree with $\tau_r = 1/D_r$ within the experimental error bars (figure 5), where

$$D_r = \frac{k_B T}{8\pi\eta R^3} \qquad (1)$$

is the rotational diffusion of the particle. This suggests that the cap reorientation is mainly due to free rotational diffusion and remains rather unaffected by the propulsion mechanism. We note that this decoupling of rotational and translational motion largely simplifies corresponding numerical simulations of this system.

The possibility of tuning the active Brownian motion of the micro-swimmers can be employed in various contexts. For example, we have harnessed the dependence of the swimming strength on the illumination intensity to investigate the behavior of a micro-swimmer in a spatial light gradient, where its swimming properties are space-dependent; these conditions resemble the situation of bacteria moving inside a chemical gradient. Figure 6(a) shows the trajectory of a micro-swimmer moving inside a radial illumination gradient; the radial dependence of the intensity is shown in figure 6(b). The particle starts from the lower left corner, where, since

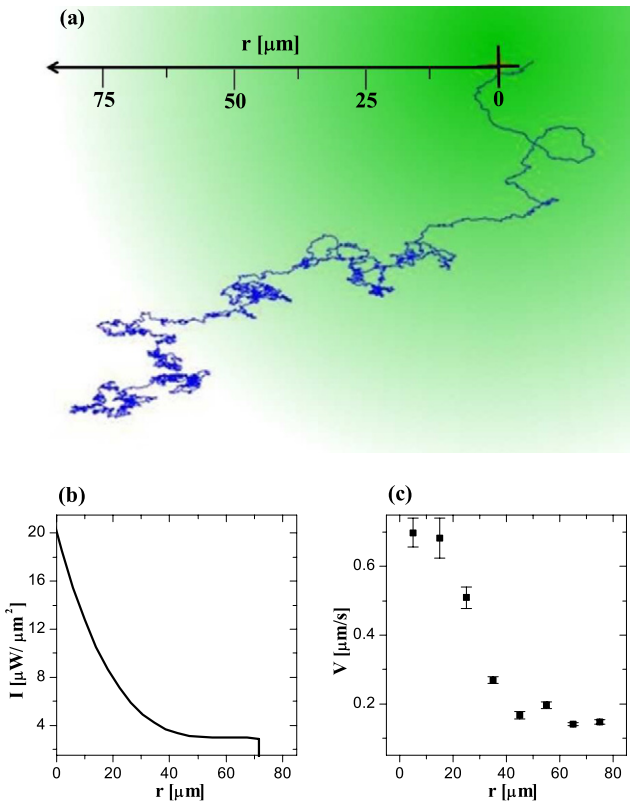

Figure 6. (a) Trajectory of a self-propelled Janus particle in a radial light gradient. (b) Intensity as a function of the radial position r. (c) Average swimming velocity v as a function of r.

there is almost no light, it undergoes standard Brownian motion. As soon as the particle randomly moves closer to the center, it starts to perform active Brownian motion with increasingly high v as it approaches the high-intensity center of the gradient; the radial dependence of v is plotted in figure 6(c). Furthermore, the trajectories become more directed and less rough as the active motion increases.

In conclusion, we have described a self-propulsion mechanism based on the local asymmetric demixing of a critical binary mixture around a microscopic Janus particle. The main advantage of this mechanism is that, since the required heating is very small (a fraction of a kelvin), the active Brownian motion can be easily tuned by a very weak illumination, which permits us to avoid optical forces acting on the highly asymmetric Janus particles. Furthermore, it is possible to control the active Brownian motion of the micro-swimmers both in space and in time by employing spatial and temporal illumination patterns.

Acknowledgments

We gratefully acknowledge D Vogt and H-J Kümmerer for their help with the experiments. This work has been partially supported by the Marie Curie-Initial Training Network Comploids, funded by the European Union Seventh Framework Program (FP7).

References

[1] Ebbens S J and Howse J R 2010 In pursuit of propulsion at the nanoscale *Soft Matter* **6** 726–38
[2] Erdmann U, Ebeling W, Schimansky-Geier L and Schweitzer F 2000 Brownian particles far from equilibrium *Eur. Phys. J.* B **15** 105–13
[3] Hänggi P and Marchesoni F 2009 Artificial brownian motors: controlling transport on the nanoscale *Rev. Mod. Phys.* **81** 387–442
[4] Berg H C 2004 *E. coli in Motion* (Heidelberg: Springer)
[5] Berg H C and Brown D A 1972 Chemotaxis in *Escherichia coli* analysed by three-dimensional tracking *Nature* **239** 500–4
[6] Matthaus F, Jagodic M and Dobnikar J 2009 *E. coli* superdiffusion and chemotaxis—search strategy, precision, and motility *Biophys. J.* **97** 946–57
[7] Weibel D B, Garstecki P, Ryan D, DiLuzio W R, Mayer M, Seto J E and Whitesides G M 2005 Microoxen: microorganisms to move microscale loads *Proc. Natl Acad. Sci. USA* **102** 11963–7
[8] Ford R M and Harvey R W 2007 Role of chemotaxis in the transport of bacteria through saturated porous media *Adv. Water Res.* **30** 1608–17
[9] van Teeffelen S and Hartmut Löwen H 2008 Dynamics of a brownian circle swimmer *Phys. Rev.* E **78** 020101
[10] Downton M T and Stark H 2009 Simulation of a model microswimmer *J. Phys.: Condens. Matter* **21** 204101
[11] Yang W, Misko V R, Nelissen K, Kong M and Peeters F M 2012 Using self-driven microswimmers for particle separation *Soft Matter* **8** 5175–9
[12] Tierno P, Golestanian R, Pagonabarraga I and Sagues F 2008 Magnetically actuated colloidal microswimmers *J. Phys. Chem.* B **112** 16525–8
[13] Ghosh A and Fischer P 2009 Controlled propulsion of artificial magnetic nanostructured propellers *Nano Lett.* **9** 2243–5
[14] Snezhko A, Belkin M, Aranson I S and Kwok W K 2009 Self-assembled magnetic surface swimmers *Phys. Rev. Lett.* **102** 118103
[15] Dreyfus R, Baudry J, Roper M L, Fermigier M, Stone H A and Bibette J 2005 Microscopic artificial swimmers *Nature* **7060** 862–5
[16] Zhang L, Abbott J J, Dong L, Peyer K E, Kratochvil B E, Zhang H, Bergeles C and Nelson B J 2009 Characterizing the swimming properties of artificial bacterial flagella *Nano Lett.* **9** 3663–7
[17] Leoni M, Kotar J, Bassetti B, Cicuta P and Lagomarsino M C 2008 A basic swimmer at low Reynolds number *Soft Matter* **5** 472–6
[18] Golestanian R, Liverpool T B and Ajdari A 2007 Designing phoretic micro-and nano-swimmers *New J. Phys.* **9** 126
[19] Paxton W F, Sen A and Mallouk T E 2005 Motility of catalytic nanoparticles through self-generated forces *Chem. Eur. J.* **11** 6462–70
[20] Vicario J, Eelkema R, Browne W R, Meetsma A, La Crois R M and Feringa B L 2005 Catalytic molecular motors: fuelling autonomous movement by a surface bound synthetic manganese catalase *Chem. Commun.* **31** 3936–8
[21] Mano N and Heller A 2005 Bioelectrochemical propulsion *J. Am. Chem. Soc.* **127** 11574–5
[22] Golestanian R, Liverpool T B and Ajdari A 2005 Propulsion of a molecular machine by asymmetric distribution of reaction products *Phys. Rev. Lett.* **94** 220801
[23] Wang Y, Hernandez R M, Bartlett D J Jr, Bingham J M, Kline T R, Sen A and Mallouk T E 2006 Bipolar electrochemical mechanism for the propulsion of catalytic nanomotors in hydrogen peroxide solutions *Langmuir* **22** 10451–6
[24] Howse J R, Jones R A L, Ryan A J, Gough T, Vafabakhsh R and Golestanian R 2007 Self-motile colloidal particles: from directed propulsion to random walk *Phys. Rev. Lett.* **99** 048102

[25] Pantarotto D, Browne W R and Feringa B L 2008 Autonomous propulsion of carbon nanotubes powered by a multienzyme ensemble *Chem. Commun.* **13** 1533–5
[26] Palacci J, Cottin-Bizonne C, Ybert C and Bocquet L 2010 Sedimentation and effective temperature of active colloidal suspensions *Phys. Rev. Lett.* **105** 088304
[27] Popescu M N, Dietrich S, Tasinkevych M and Ralston J 2010 Phoretic motion of spheroidal particles due to self-generated solute gradients *Eur. Phys. J.* E **31** 351–67
[28] Jiang H R, Yoshinaga N and Sano M 2010 Active motion of a Janus particle by self-thermophoresis in a defocused laser beam *Phys. Rev. Lett.* **105** 268302
[29] Volpe G, Buttinoni I, Vogt D, Kümmerer H J and Bechinger C 2011 Microswimmers in patterned environments *Soft Matter* **7** 8810–5
[30] Grattoni C A, Dawe R A, Seah C Y and Gray J D 1993 Lower critical solution coexistence curve and physical properties (density, viscosity, surface tension, and interfacial tension) of 2,6-lutidine + water *J. Chem. Eng. Data* **38** 516–9
[31] Binder K and Stauffer D 1974 Theory for the slowing down of the relaxation and spinodal decomposition of binary mixtures *Phys. Rev. Lett.* **33** 1006–9
[32] Wong N C and Knobler C M 1981 Light-scattering studies of phase separation in isobutyric acid + water mixtures: hydrodynamic effects *Phys. Rev.* A **24** 3205–11
[33] Gerold V and Kostorz G 1978 Small-angle scattering applications to materials science *J. Appl. Crystallogr.* **11** 376–404
[34] Snyder H L, Meakin P and Reich S 1983 Dynamical aspects of phase separation in polymer blends *Macromolecules* **16** 757–62
[35] Hashimoto T, Itakura M and Hasegawa H 1986 Late stage spinodal decomposition of a binary polymer mixture. I. Critical test of dynamical scaling on scattering function *J. Chem. Phys.* **85** 6118–28
[36] Palik E D 1985 *Handbook of Optical Constants of Solids* (Orlando, FL: Academic)
[37] Baffou G, Quidant R and Girard C 2009 Heat generation in plasmonic nanostructures: influence of morphology *Appl. Phys. Lett.* **94** 153109
[38] Girard G 2005 Near field in nanostructurs *Rep. Prog. Phys.* **68** 1883–933
[39] Franke K and Gruler H 1990 Galvanotaxis of human granulocytes: electric field jump studies *Eur. Biophys. J.* **18** 334–46